BULK PROPERTIES OF PLUTO AND CHARON

DAVID J. THOLEN
University of Hawaii

and

MARC W. BUIE
Lowell Observatory

Much of what we can deduce about the origin and evolution of the Pluto–Charon system, and its implications for the outer solar system, depends on our knowledge of the bulk properties of the two bodies. In this chapter, we review the inventory of the system; the orbits of the two bodies; their rotational states, sizes, masses and densities; other global surface characteristics; and their atmospheres. Historically significant improvements to these various parameters are mentioned, and we attempt to assess the reliability of the latest values and reach a consensus where possible. Key quantities include a 6.38726±0.00007 day rotational period for Pluto, a 6.387223±0.000017 day orbital period for Charon, an orbital semimajor axis of 19,636±8 km and significant nonzero eccentricity for Charon, a system mass of 0.002433±0.000003 Earth masses, a consensus Charon–Pluto mass ratio of 0.119±0.005, a Pluto radius between 1145 and 1200 km, a Charon radius between 600 and 650 km, a system mean density between 1.87 and 2.03 g cm^{-3}, a Pluto density between 1.92 and 2.06 g cm^{-3}, and a Charon density between 1.51 and 1.81 g cm^{-3}. The surface composition of Pluto includes the spectroscopically detected ices of methane, nitrogen, carbon monoxide, and water, whereas only water ice has been detected on Charon. The composition of Pluto's atmosphere is apparently dominated by nitrogen, with much smaller amounts of methane and carbon monoxide; no detectable atmosphere has been found around Charon.

I. INTRODUCTION

Our knowledge of the Pluto–Charon system has grown tremendously during the past two decades, driven primarily by the discovery of Charon in 1978 and the realization that during the 1980s, the orbit of Charon would be viewed sufficiently close to edge-on from the Earth so as to produce a lengthy series of mutual occultation and eclipse events. These events offered a rare opportunity to perform observations that would answer some long-standing questions about the surface compositions, sizes, albedos, and density of the system. In addition, a stellar occultation permitted the first real measurements of the atmosphere around Pluto in 1988. More recent advances in infrared instrumentation have permitted the acquisition of spectra with unprecedented resolution, which have led to further improvements in our knowledge of the surface composition. Furthermore, the launch of the Hubble Space Telescope (HST) provided new opportunities for high angular resolution studies of the system. All of these factors combined to revolutionize our knowledge of the solar system's outermost planet.

This chapter summarizes what has been learned about the bulk properties of the system, including some of the historical development that preceded modern measurements. The best values of the various parameters discussed in detail in the following sections can be found for convenience in Table I.

II. SYSTEM INVENTORY

Closer examination of the outer planets by spacecraft has in each case led to the discovery of additional satellites, though they have all been small and in close orbits, where detection from Earth is the most difficult, due to scattered light from the primary body. In the case of Pluto, the volume of space around the planet that is stable against solar perturbations extends to approximately 100 Charon orbit radii (about 90 arcsec), and given that Charon escaped detection until 1978, it seemed possible that other small satellites might have similarly eluded astronomers. Deep CCD surveys by Stern et al. (1991*b*) failed to detect any additional satellites down to magnitude 20.6 in the region from 6 to 10 arcsec from Pluto, and to magnitude 22.6 beyond that, extending to the limit of the stability region. For an assumed albedo of about 0.4, these magnitude limits correspond to radius upper limits of 58 ± 19 km and 23 ± 8 km, respectively.

To address the question of additional satellites in close orbits, Stern et al. (1994) utilized archival Hubble Space Telescope images of the Pluto–Charon system to examine the region from 0.1 to 10 arcsec from Pluto. At the 90 percent confidence level, no additional satellites were detected brighter than magnitude 19.3 at the smaller separations, dropping to magnitude 21.9 at the larger separations. The corresponding radius limits are 140 km and 42 km for the same assumed albedo as for the earlier study. Dynamical considerations led to the conclusion that low-inclination, prograde orbits in the region from about half of Charon's semimajor axis (a) to twice that value are unstable. The instability region extends from $0.65a$ to $1.6a$ for retrograde orbits.

III. ORBITS

Pluto lies so far from the Sun that its motion on the sky is quite slow. As a result, it took a relatively long time to determine a reliable heliocentric orbit for the system, a situation that is being repeated in current times with each new trans-Neptunian object that is discovered. Unlike the present situation, however, there was little appreciation for orbital resonances in the outermost part of the solar system back in the 1930s, so the earliest orbit solutions for Pluto were often unconstrained. As a result, some of those early solutions

TABLE I

Bulk Properties of the Pluto–Charon System

Quantity		System	Pluto	Charon
Rotational period (days)		—	6.38726±0.00007[a]	Consistent with orbit[b]
Radius (km)[c]		—	1145 to 1200	600 to 650
Mass (10^{25}g)[d]		1.471±0.002	1.315±0.003	0.156±0.003
Density (g cm^{-3})[e]		1.87 to 2.03	1.92 to 2.06	1.51 to 1.81
Surface gravity (m s^{-2})[f]		—	0.66	0.29
Surface composition		—	H_2O, N_2, CH_4, CO ices[g]	H_2O ice[h]
Atmospheric composition		—	N_2, CH_4, CO[g]	?[i]
Pressure scale height (km)[j]		—	55.7±4.5	—
Phase coefficient (mag deg^{-1})		0.0372±0.0016[a]	0.0294±0.0011[b]	0.0866±0.0078[b]
Temperature (K)[k]		—	40±2	?
Lightcurve (mag)	(1954)[l]	0.11	—	—
	(1964)[m]	0.15	—	—
	(1972)[n]	0.22[p]	—	—
	(1984)[a]	0.30	—	—
	(1993)[b]	—	0.33	0.08
Blue albedo[o]		—	0.44 to 0.61	0.38
$B - V$ color index (mag)[p]		0.843±0.008	0.867±0.008	0.700±0.010
Semimajor axis		39.544674 AU[q]	—	19636±8 km[r]
Eccentricity		0.249050[q]	—	0.0076±0.0005[r]
Inclination (deg)		17.14217[q,s]	—	96.163±0.032[r,t]
Ascending node (deg)		110.29714[q,s]	—	222.993±0.024[r,t]
Longitude of periapsis (deg)		224.13486[q,s]	—	219.1±0.9[r,t]
Mean longitude (deg)		238.74394[q]	—	32.875±0.023[r]
Epoch		JDT 2451545.0[q]	—	JDT 2449000.5[r]
Period		248.0208 yr[q]	—	6.387223±0.000017 day[r]
Obliquity (deg)		119.6±0.6[u]	—	—

[a] Tholen and Tedesco (1994); the phase coefficient is for a wavelength of 0.44 μm; [b]Buie et al. (1997); the phase coefficients are for a wavelength of 0.55 μm. [c]The values given here represent the range of possible values from multiple inconsistent determinations, including a standard deviation on either side. See the text for more detail. [d]The system mass was derived from Tholen and Buie (1997), and the individual masses were derived using the consensus mass ratio presented in this chapter. [e]The density ranges are based on the masses and radius ranges given in this table. [f]The surface gravity is derived from the mass and radius values given in this table. [g]Owen et al. (1993,1997). [h]Buie et al. (1987); Marcialis et al. (1987). [i]Elliot and Young (1991). [j]Elliot and Young (1992). [k]Tryka et al. (1994); temperature refers to nitrogen frost on Pluto, with planet at 29.7 AU from the Sun. [l]Walker and Hardie (1955). [m]Hardie (1965). [n]Andersson and Fix (1973). [o]Tholen and Buie (1990). [p]Binzel (1988). [q]Anonymous (1992). [r]Tholen and Buie (1997). [s]Referred to mean ecliptic and equinox of J2000.0. [t]Referred to mean equator and equinox of J2000.0. [u]Derived from the two orbits given here.

yielded what would now be considered as unlikely, if not ridiculous, orbits, including strongly hyperbolic ones (see the chapter by Reaves).

After the inclusion of prediscovery astrometric observations from the mid-1910s, however, the true nature of Pluto's orbit became fairly well established. The mean orbital elements, as they are presently known, are shown in Table I, for which the reference frame is the mean ecliptic and equinox of J2000. Note that Pluto has been observed for only approximately one-third of its 248-yr orbit, so the orbit determination is the least accurate of the major planets. The ephemeris uncertainty is less than about 0.2 arcsec at the present epoch, however.

Pluto stands out from the rest of the planets by having both the highest eccentricity and inclination. In fact, the eccentricity is sufficiently large that for about 20 years out of each 248-yr orbit, Pluto can get closer to the Sun than Neptune. Despite the fact that the orbits of Neptune and Pluto cross when projected onto the ecliptic plane, Pluto never gets very close to Neptune. Indeed, Pluto passes closer to Uranus than it does to Neptune. The reason for this interesting situation is the 2:3 resonance between the mean motions of Pluto and Neptune; that is, Pluto orbits the Sun twice for every three orbits by Neptune (Cohen and Hubbard 1965; Applegate et al. 1986). A possible origin for this condition has been discussed by Malhotra (1995). Both Neptune and Pluto may have originally been in circular, nonresonant orbits around the Sun. While Neptune was migrating outward during the epoch of planetesimal clearing in the giant planet region, it could have trapped Pluto into the 2:3 resonance. For more details, see the chapter by Malhotra and Williams. Despite the persistence of the 2:3 resonance, the long-term behavior of Pluto's orbit has been shown as chaotic (Sussman and Wisdom 1988), with an *e*-folding time of only 20 Myr.

The orbit of Charon is a story that has unfolded much more recently. The early interest in that orbit was due to its ability to provide a measure of the system's total mass, a quantity that had been subject to much speculation (see Sec. VI). In addition, knowledge of the orbit of Charon was crucial to predicting the times that the mutual occultation and eclipse events would occur. As a result, considerable effort was expended to determine that orbit during the time between the discovery of Charon in 1978 and the expected onset of the mutual event season in the early 1980s.

The first orbit solution for Charon was published by Christy and Harrington (1978) in the paper that described the discovery of Charon. That solution was based on a handful of position angle and separation measurements extracted from photographic plates of the system. After additional images of Charon were secured, an improved orbit was published (Harrington and Christy 1980). In 1980, the first speckle interferometric observations of the system were made, and those observations were utilized for yet another improved determination of the orbit (Harrington and Christy 1981). After additional speckle observations of the system became available, it soon became clear that systematic differences between the various data sets existed, presumably due to the techniques used to calibrate the image scale and the direction of north, to which position angles are referred (Tholen 1985). So when Beletic et al. (1989) endeavored to acquire speckle observations for a complete orbit in 1985, particular attention was paid to both the image scale and position angle calibrations. The resulting orbital radius of 19640±320 km has been extensively used since then (see Sec. V).

Once a sufficient number of mutual events had been observed (see the chapter by Binzel and Hubbard), it became possible to determine the orbit of Charon independently of the astrometric observations, though the orbital radius could be stated only in units of the two objects' radii rather than in absolute units. Annual improvements to the orbit determination were made after each opposition's observations were added to the analysis, with the latest published by Tholen and Buie (1990). The mutual event technique is particularly powerful in determining the longitude of the ascending node, the mean longitude, and the orbital period, but less powerful in determining the inclination of the orbit. Because the time interval between events could be measured quite accurately, the mutual events were also quite sensitive to any orbital eccentricity for orientations of the line of apsides that were not aligned with the line of sight to the system. Although the relative duration of inferior (Charon in front of Pluto) and superior (Charon behind Pluto) events could be used to constrain the eccentricity for apsidal orientations that were aligned with the line of sight, that constraint was much weaker, due to the event durations' correlation with the radius determinations for Pluto and Charon. The upper limit on the eccentricity was only about 10^{-2} in this case (Tholen and Buie 1989), whereas orbit solutions that had the longitude of periapsis constrained to not lie along the line of sight were able to place a much tighter upper limit of about 10^{-3} on the orbital eccentricity (Tholen and Buie 1990). Even longer numerical integrations of Pluto's orbit have been computed in recent years; for the details, see Table II in the chapter by Malhotra and Williams.

Although the orbit of Charon had been fairly well established by the end of the mutual event season, two problems remained. First, the absolute radii of Pluto and Charon depended on knowledge of the orbital semimajor axis in absolute units, for which the speckle orbit of Beletic et al. (1989) was still being utilized. The quality of the mutual event observations was such that the uncertainties in the radius determinations were being dominated by the uncertainty in the semimajor axis, which was about one part in sixty. Second, the orbit solution only provided the total mass of the system, which made it impossible to compute the individual densities of Pluto and Charon, even though their individual radii were now known. As a result, new observations were undertaken in the early 1990s to answer these outstanding questions. More details about these observations are in Sec. VI.

One of those experiments, however, led to a surprising result: a significant nonzero eccentricity was found (Tholen and Buie 1997). The formal result for the orbit of Charon's center of light around Pluto's center of light yielded an eccentricity of 0.0076±0.0005, with the line of apsides nearly aligned along the line of sight from Earth, which is the orientation to which the mutual events were least sensitive. The surface albedo distribution on Pluto, and possibly on Charon as well, could produce an offset in the center of light from the center of the disk, however, thereby affecting the eccentricity determination. Nevertheless, when models of the surface albedo distributions are imposed on the orbit solution, only about half of the eccentricity can be accounted for, leaving a significant nonzero amount. Given that tidal effects can damp out such an orbital eccentricity on a time scale of 1 to 10 Myr, depending on the dissipation function, either the system was disturbed relatively recently, or some mechanism is responsible for sustaining a nonzero eccentricity. See the chapter by Dobrovolskis et al. for more discussion of the tidal interaction between Pluto and Charon.

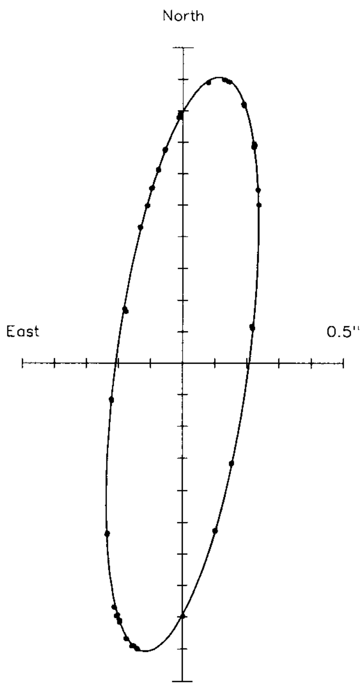

Figure 1. The orbit of Charon, based on sixty images of the system obtained with the Hubble Space Telescope in 1992 and 1993.

The average insolation for a given point on Pluto's surface depends on the obliquity of the spin axis. Tidal effects should have also caused that spin axis to be parallel to Charon's orbital angular momentum vector, though the existence of a nonzero eccentricity suggests the possibility of a slight difference. If we ignore a possible small difference, however, the latest orbit of Charon implies an obliquity of 119.61 deg. The accuracy of this value depends on the accuracy with which the orbital inclination and ascending node are known for both the system's heliocentric orbit and Charon's orbit. In this case, the limiting factor is the accuracy of Charon's inclination. Although the formal uncertainty in this value is rather small, there are still some unexplained discrepancies between the various inclination determinations; thus, the true uncertainty is probably at least several tenths of a degree, and possibly more than a degree. For purposes of Table I, we have adopted an error bar of 0.6 deg, which encompasses all the recent observations at the 2σ level. A summary of the various orbit determinations for Charon is shown in Table II, and Fig. 1 shows the orbit determination by Tholen and Buie (1997).

IV. ROTATIONS

The first time series of photometric observations of Pluto were made by Baade (1934). He noted possible variation of 0.2 mag, based on one night of data (1933 October 14) that yielded systematically brighter magnitudes for Pluto than the adopted mean. The peak-to-peak scatter in the two nights of data from 1933 March, however, was 0.18 mag, probably due to the limited precision of the photographic technique utilized for the observations. Thus it is difficult to determine what the true rotational lightcurve variation might have been at this early epoch. Baade made no attempt to derive a rotational period from his observations.

It would take two more decades, after the introduction of photomultiplier tubes, before brightness measurements with sufficient precision to detect real rotational variation would be made. Although Kuiper was the first to attempt photoelectric measurements of Pluto, he never independently published those results. All that ever made it into the literature were six of his 1953 observations, which were included in a paper describing observations in 1954 and 1955 by Walker and Hardie (1955). Using all three years of data, they were able to deduce a rotational period of 6.390 ± 0.003 days from brightness variations of about 0.11 mag. Interestingly, they believed Pluto was being viewed nearly equator-on, because of the large amount of variation seen. We now know that Pluto was much closer to a solstice at that time.

It appears that more Pluto lightcurve observations were not attempted until 1964, when Hardie (1965) attempted to improve on the earlier results. The accuracy of his new rotational period determination (6.38673 ± 0.00030 days) was noted to be ten times higher, thanks to the decade-long time base. He noted a slight increase in the amount of brightness variation (then up to about 0.15 mag) and a possible decrease in the mean brightness, but questioned the absolute calibrations of the two data sets and therefore the significance of this latter point. Interestingly, he apparently suggested to a reporter that Pluto was appreciably limb darkened, because otherwise the lightcurve asymmetry could be explained "only by an extremely unlikely pattern of dark and bright

TABLE II

Summary of Charon Orbit Determinations (Epoch 1993 January 13.0 TT)[a]

a (km)	e	i (deg)	Ω (deg)	$\tilde{\omega}$ (deg)	L (deg)	P (days)	Reference
17400	[0.0]	105.0[b]	350.0[a]	—		6.3867	Christy and Harrington (1978)
20000	[0.0]	105.0[b]	170.0[b]	—		6.3867	Harrington and Christy (1980)
19700	[0.0]	94.00[c]	221.0[c]	—	75.00[d]	6.3871	Harrington and Christy (1981)
300		9	7		1.2	18	
19360	[0.0]	93.9[c]	219.8[c]	—	76.6[d]	6.38764	Tholen (1985)
320		9	21		93	35	
19640	[0.0]	98.5[e]	222.96[e]	—	32.96	6.387219	Beletic et al. (1989)
	21	1.0	24	31	25	11	
[19640]	0.00020	99.1[e]	223.015[e]	73[e]	32.34	6.387246	Tholen and Buie (1990)
86		26	41		24		
19405	[0.0]	96.56[e]	223.007[e]	—	32.58	[6.387246]	Null et al. (1993)
58		24					
19460	[0.0]	95.00[e]	[223.01][e]	—	[32.34]	[6.387246]	Young et al. (1994)
81	67	24		35	49		
19662	0.0072	96.57[e]	[223.015][e]	2[e]	33.15	[6.387246]	Null and Owen (1996)
8	5	32	24	2.2	47	17	
19636	0.0076	96.163[e]	222.993[e]	219.1[e]	32.875	6.387223	Tholen and Buie (1997)

[a] Values in brackets were assumed; error bars are shown above each value in units of the last digit (where available).
[b] Referred to plane of the sky.
[c] Referred to the mean equator and equinox of B1950.0.
[d] True anomaly.
[e] Referred to the mean equator and equinox of J2000.0.

surface markings" (Anonymous 1965). No explanation was provided for how limb darkening could produce the asymmetric lightcurve exhibited by Pluto.

Andersson and Fix (1973) apparently had more confidence in the brightness decrease that Hardie questioned. Such variation can be used to constrain the orientation of an object's spin axis, so they set out to acquire additional lightcurve data at a new epoch. The new brightness measurements, made between 1971 and 1973, revealed a still fainter mean magnitude, with the amount of variation up to 0.22 mag. The rotational period used in their analysis was 6.3867 days, though it appears that they simply adopted the solution of Hardie (1965) rather than solving for the period themselves. The trend toward a fainter and more variable Pluto was now clearly established, and to explain the decreasing brightness, they proposed that "the polar regions of the planet have a higher albedo than do its equatorial regions." They solved for a region in which they believed the pole to lie, which turns out to be fairly close to the pole location as it is known today.

Kiladze (1966) re-analyzed the 1953–1955 photometry and reported that a period of 1.1819 days could also satisfy the observations. That uncertainty prompted Neff et al. (1974) to make new, higher-time-resolution observations in 1973 to resolve the matter. Their data were sufficient to reject the shorter period and further refined the rotational period to be 6.38737±0.00018 days.

Motivation for additional observations of Pluto was provided after the discovery of Charon in 1978 and the confirmation that the epoch of mutual events was just about to start, rather than having just ended (Andersson 1978). To detect the earliest events, which would be quite shallow, it was necessary to know the intrinsic lightcurve of the system to both high photometric accuracy and longitudinal resolution. That need prompted a four-year-long study of the lightcurve spanning 1980–1983 by Tholen and Tedesco (1994), as well as a two-year-long study spanning 1982 to 1983 by Binzel and Mulholland (1983,1984). Both found the amount of variation to have increased still more, to about 0.3 mag, and confirmed that the mean brightness of the system had continued to decline. Tholen and Tedesco determined the rotational period to be 6.38726±0.00007 days from the 1980–1983 data alone; no attempt was made to link the older observations to the newer ones, given the evolution of the lightcurve amplitude and shape.

Observations of Pluto's lightcurve by Lyutyi and Tarashcuk (1982,1984) were apparently motivated by the planet's approach to perihelion in 1989. Their rotational period determination utilized the data extending back to the 1950s, however, and apparently suffers from changes in the sub-Earth longitude corresponding to minimum light as a function of sub-Earth latitude, given that they found 6.38663±0.00006 days, which differs from the Tholen and Tedesco period determination by 6.8σ.

Although the observations described above were of the integrated light from the Pluto–Charon system, they were treated as representing the rotational period of Pluto, given that Charon did not contribute enough light to the total (Reitsema et al. 1983) to produce variation as large as 0.3 mag. Confirmation

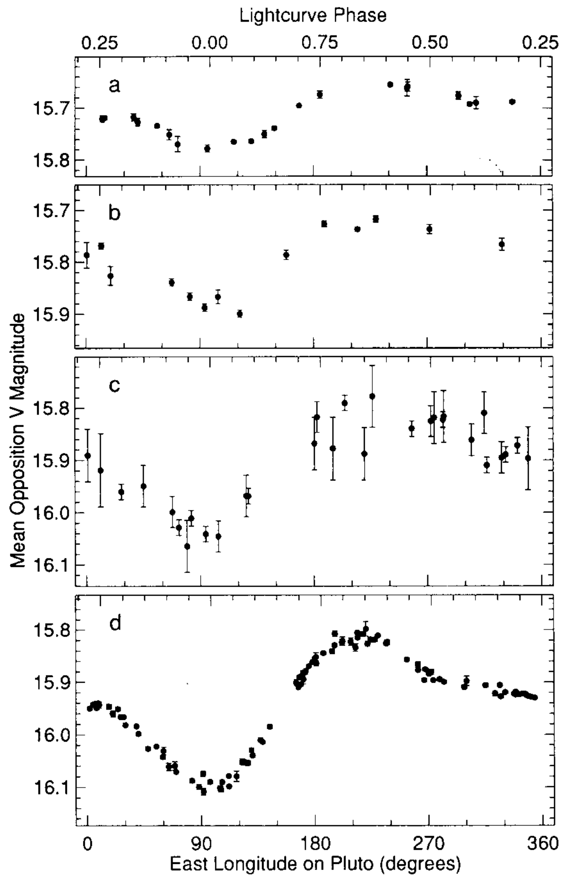

Figure 2. Representative rotational lightcurves from each of the last four decades. (a) Data from 1953 to 1955 (Walker and Hardie 1955). (b) Data from 1964 (Hardie 1965). (c) Data from 1971 to 1973 (Andersson and Fix 1973). (d) Data from 1980 to 1983 (Tholen and Tedesco 1994).

of this fact came from those mutual events during which Charon was completely hidden behind Pluto. Those portions of the lightcurve showing only Pluto still exhibited essentially the same slope as the system lightcurve.

The lightcurve of Charon is much harder to measure from groundbased telescopes, due to the difficulty in removing the contribution of Pluto from the total. Although photometric variability in Charon's light had been detected at infrared wavelengths (Bosh et al. 1992), an independent rotational period could not be established. On the other hand, Buie and Shriver (1994) showed that the technique used by Bosh et al. does not work very well. Instead, theoretical arguments based on tidal dissipation calculations have been used to conclude that Charon's rotational period must be the same as Pluto's (Farinella et al. 1979; see also the chapter by Dobrovolskis et al.). The only observational evidence to support this theoretical conclusion came from observations made with the HST (Buie et al. 1997). The slight 0.08 mag variation seen in visible light is consistent with synchronous rotation.

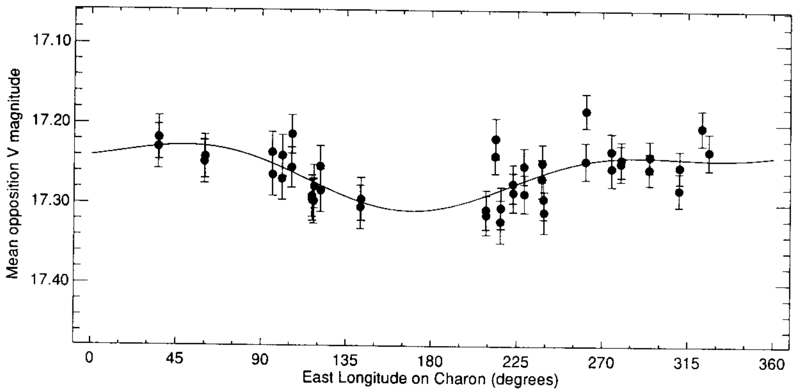

Figure 3. The rotational lightcurve of Charon, extracted from the same data set used to determine the orbit shown in Fig. 1.

Figure 2 shows representative rotational lightcurves from each of the last four decades, and Fig. 3 shows the lightcurve of Charon, plotted under the assumption that it rotates synchronously.

V. SIZES

The sizes of Pluto and Charon have been measured in a variety of ways. Indirect techniques, such as taking the observed brightness and assuming a geometric albedo, will not be discussed here. Instead, attention will be focused on more direct techniques, such as stellar occultations, speckle interferometry, direct imaging, and mutual event photometry.

Prior to the discovery of Charon, Kuiper (1950) attempted to measure the size of Pluto using a diskmeter. The earliest attempts in 1948 with the McDonald 2.1-m telescope failed, but the night of 1949 November 4 yielded exceptional seeing, and a diameter of 0.4 arcsec was independently determined by two different observers. Because the observation was deemed to be at or beyond the threshold of the telescope's capability, Kuiper made arrangements to use the instrument on the 5-m Hale telescope at Palomar the following year. The observation on 1950 March 22 yielded a diameter of 0.23±0.01 arcsec and was confirmed by a second observer. Kuiper was uncertain whether the effect of a corrector lens should be applied, which would have reduced the diameter to 0.20±0.01 arcsec. He adopted the larger result, however, which corresponded to a linear diameter of 5900 km. It is worth noting that unlike the McDonald Observatory experiment, "it was established beyond doubt that the 200-inch result was a real measure and not merely an upper limit," and Kuiper later went on to write that "the diameter measurement is so comparatively simple and direct that the possibility of a serious systematic error seems excluded." Clearly some systematic error was present, given that his result is now known to be a factor of 2 too large, quite possibly due to the presence of Charon, though there is no mention of a second object being seen or even the possibility of one in Kuiper's paper. On both nights, however, the separation between Pluto and Charon was about 0.65 arcsec, with Charon on nearly opposite sides of Pluto for the two observations. It is also not clear how Kuiper was able to measure a planetary disk of only 0.20 arcsec diameter, given that the atmospheric seeing at even the best terrestrial observatory sites is rarely better than about 0.5 arcsec. Only with modern adaptive optics systems has groundbased visible-light resolution reached such small values.

A particularly powerful technique for measuring the diameters of small solar system objects is via stellar occultations. Unfortunately, Pluto moves so very slowly on the sky that occultation opportunities are comparatively rare, and its small angular diameter makes the accurate prediction of the occultation path that much more difficult. If an occultation observation does not yield an event, all one can do is place an upper limit on the size of the occulting body. Such was the case for the 1965 occultation observed by Halliday et al. (1966), for which a comparatively uninteresting 2σ upper limit of 6800 km was derived; if the astrometry is without error, then the radius limit is about 5500 km. The 1980 occultation opportunity seems to have been largely ignored. Only one successful observation was obtained (Walker 1980), and the astrometry indicated that the occulting body was not Pluto, but rather Charon. The chord length of 50 sec combined with a sky plane velocity of 24.076 km s^{-1} yielded a lower limit for Charon's diameter of 1200 km. A more recent re-analysis of the data from this event by Elliot and Young (1991) placed the 3σ lower limit at 1203 km.

Similarly, the 1985 occultation by Pluto was observed at only one site, and that one was under adverse conditions (Brosch 1995), which raised serious doubts about the validity of the observation. The data for this event are at best indicative of grazing geometry, so any lower limit on the diameter of Pluto that could be derived from the data is relatively uninteresting (see the chapter by Binzel and Hubbard). Of more interest is the possible detection of an atmosphere, which is discussed in more detail in Sec. VIII.

The first (and only) stellar occultation event that was useful for purposes of measuring the size and shape of Pluto occurred in 1988 (Millis et al. 1993). Unfortunately, the presence of an atmosphere, and some uncertainty over the proper interpretation of the data's departure from what one would expect for an isothermal atmosphere, have made an unambiguous surface radius determination difficult, though some useful constraints can be placed on that radius. If the atmosphere is assumed to be clear, then the fitted surface radius is 1195$\pm$5 km, but if the atmosphere has a haze layer, then the surface radius falls somewhere below 1180$\pm$5 km. In an independent interpretation by Stansberry et al. (1994), a temperature inversion was hypothesized that can both reproduce the observed lightcurves and hide a troposphere of significant depth. Their models allow a surface radius for Pluto as low as 1158 km, which is formally consistent with those derived from mutual event modeling (see below). Although the surface radius is clearly model dependent, the radius at which the light from the occulted star reached the 76.4% flux level was rather accurately determined to be 1274.4±4.6 km.

Speckle interferometry has been utilized in an attempt to measure the diameters of Pluto and Charon, though with limited success. The first attempt was made by Arnold et al. (1979), who derived a diameter of 3000±400 km assuming no limb darkening, or 3600±400 km assuming a cosine limb darkening law. Interestingly, the observations were made before the discovery of Charon; one might expect a technique that was able to resolve the disk of Pluto to have easily revealed Charon. Their paper was published after the Charon discovery announcement, however, and they indicate knowledge of that discovery, yet no results for Charon were mentioned. Bonneau and Foy (1980) found Pluto's diameter to be 4000±400 km and Charon's to be 2000±200 km; although we now know that these values are much too large, the ratio of the two diameters is in excellent agreement with the mutual event results, which seems indicative of some sort of systematic error. Baier and Weigelt (1987) determined that Pluto's diameter was between 2710 and 3460 km, depending on the assumed magnitude difference between the two objects and whether a cosine limb darkening law was assumed. The corresponding results for Charon were between 1050 and 1520 km.

The radii of Pluto and Charon have also been fitted to direct images obtained with the HST's Faint Object Camera (Albrecht et al. 1994). The result for Pluto is 1160 km, for both the F550M and F342W filters, though the fitted value for the limb darkening coefficient is less for the latter filter. For Charon, the limb darkening parameters are the same for the two filters, though the fitted radii are 650 and 635 km, respectively. Both Albrecht et al. and Young and Binzel (1994) find Charon to be more limb darkened than Pluto, though in the former authors' case, the difference is marginal. It seems unusual that the lower albedo object would be more limb darkened.

The remaining radius determinations have resulted from the modeling of mutual event data. The most recent determinations by Tholen and Buie (1990) yielded 1151±6 km for Pluto and 593±13 km for Charon, whereas Reinsch et al. (1994) found 1151±4 km and 591±5 km, respectively, from their data. Buratti et al. (1995) observed fifteen events, but restricted their modeling to four events that had more extensive coverage than the others. Using the approach of Dunbar and Tedesco (1986), they derived radii of 1155±20 km and 612±30 km, respectively. None of these teams attempted to include the effects of limb darkening on the fitted radii, whereas Young and Binzel (1994) did, and their results are understandably larger at 1178±23 km and 628±21 km, respectively. Because the dimensions in terms of absolute units depend on the adopted semimajor axis for Charon's orbit, all the mutual event determinations mentioned here have been scaled to the same adopted semimajor axis of 19636 km. For more information about the mutual event season, see the chapter by Binzel and Hubbard.

A summary of the various radius determinations is presented in Table III. To permit a valid comparison, all the various mutual-event-based results in this table have been scaled to the same 19636 km semimajor axis.

The shapes of Pluto and Charon have not received much treatment in the literature. Marcialis (1985) assumed a lithosphere of methane and that the temperature-viscosity law for water ice could be applied to methane to conclude that Pluto could support "only slightly rolling topography." Features larger than about 10 km were not expected to persist for more than a billion years. Given more recent developments regarding the surface ices on Pluto, this result may no longer be valid. See the chapter by Cruikshank et al. for more speculation about the topography of Pluto.

VI. MASSES AND DENSITIES

The first mass estimates for Pluto were made even before the planet's discovery. Those estimates were based on the perturbations the presumed ninth planet was having on Uranus, which figured prominently in the predictions and searches for that planet. The analyses by Pickering and Lowell yielded masses ranging from two to eleven Earth masses (see the chapter by Reaves).

Downward revisions to Pluto's mass started occurring after discovery, when the unexpected faintness of the planet led to corresponding reductions in the size estimates (see Duncombe and Seidelmann 1980 for a more thorough review). Following the discovery of methane in the spectrum of Pluto (Cruikshank et al. 1976), the implied high albedo and low density led to yet another drastic reduction in the mass estimate for Pluto. In fact, the downward trend was so noticeable that Dessler and Russell (1980) made a tongue-in-cheek prediction that the mass of Pluto would soon become negative.

Of course, the earliest mass estimates were flawed because of the incorrect assumption that a ninth planet was responsible for the observed residuals in the orbit of Uranus. Those residuals can now be attributed to systematic errors in the star catalogs used to reduce the astrometric observations and an imprecise mass for Neptune (Standish 1993). The more recent mass estimates for Pluto were more realistic, thanks to upper limits on the radius of Pluto imposed by stellar occultation observations that failed to detect Pluto (Halliday et al. 1966) and realistic density restrictions. Nevertheless, even these more realistic mass estimates were uncertain by at least an order of magnitude, due to the range of radii and densities that were compatible with the data available at the time.

The first accurate mass computations were made possible by the discovery of Charon in 1978 (Christy and Harrington 1978). Measurements of the orbital radius and period of Charon, plus the application of Kepler's third law, provide a direct determination of the total system mass. All of the modern mass determinations have used this approach, given that there has not yet been a spacecraft flyby of the planet, which is a mass measurement technique that has been used quite successfully for the other planets. Because the orbital period

TABLE III
Summary of Radius Determinations

Method	Pluto	k^a	Charon	k^a	Reference
Diskmeter	2950±130 km	—	—	—	Kuiper (1950)
Occultation[b]	<3400 km	—	—	—	Halliday et al. (1966)
Occultation[c]	—	—	>601.5 km	—	Elliot and Young (1991)
Occultation[d]	1195±5 km	—	—	—	Millis et al. (1993)
Occultation[e]	<1180±5 km	—	—	—	Millis et al. (1993)
Speckle	1500±200 km	0.5	—	—	Arnold et al. (1979)
Speckle	1800±200 km	1.0	—	—	Arnold et al. (1979)
Speckle	2000±200 km	0.5	1000±100 km	0.5	Bonneau and Foy (1980)
Speckle[f]	1355 km	0.5	645 km	0.5	Baier and Weigelt (1987)
Speckle[g]	1590 km	1.0	760 km	1.0	Baier and Weigelt (1987)
Speckle[h]	1475 km	0.5	525 km	0.5	Baier and Weigelt (1987)
Speckle[i]	1730 km	1.0	620 km	1.0	Baier and Weigelt (1987)
Mutual events	1151±6 km	[0.5]	593±13 km	[0.5]	Tholen and Buie (1990)
Mutual events	1151±4 km	[0.5]	591±5 km	[0.5]	Reinsch et al. (1994)
Mutual events	1178±23 km	0.49±0.02	628±21 km	1.02±0.08	Young and Binzel (1994)
Mutual events	1155±20 km	[0.5]	612±30 km	[0.5]	Buratti et al. (1995)
Direct imaging[j]	1160±12 km	0.6	650±13 km	0.65	Albrecht et al. (1994)
Direct imaging[k]	1160±12 km	0.55	635±13 km	0.65	Albrecht et al. (1994)

[a] Minnaert limb darkening coefficient, in brackets when implicitly assumed.
[b] 95% confidence upper limit.
[c] 3σ lower limit, where σ is 0.8 km.
[d] Assumes clear atmosphere with thermal gradient model.
[e] Assumes haze layer model.
[f] Assumes 1.6 mag difference, equal albedos, no limb darkening.
[g] Assumes 1.6 mag difference, equal albedos, limb darkening.
[h] Assumes 2.2 mag difference, equal albedos, no limb darkening.
[i] Assumes 2.2 mag difference, equal albedos, limb darkening.
[j] F550M filter; error bar does not include uncertainty in limb darkening coefficient.
[k] F342W filter; error bar does not include uncertainty in limb darkening coefficient.

was much easier to measure than the orbital radius, all of the improvements in the mass determination since 1978 have come from improvements to our knowledge of Charon's orbital radius.

The evolution in our knowledge of Charon's semimajor axis was described earlier in this chapter. The adopted value of 19636$\pm$8 km, coupled with an orbital period of 6.387223 days, yields a system GM of 981.5$\pm$1.1 km^3 s^{-2}. Expressed in inverse solar masses, the result is 135,210,000$\pm$160,000. Expressed in units of Earth masses, the result is 0.002433$\pm$0.000003. Surprisingly, the Pluto system has less than one four thousandth the mass deduced by Lowell and certainly could not have been responsible for the apparent perturbations in the orbit of Uranus. The predictions of the ninth planet's position therefore suffered from a serious flaw. That Pluto was actually found somewhere near Lowell's prediction is sheer coincidence, and credit for the planet's discovery is due more to Lowell's persistence (and Slipher's following Lowell's death), plus Tombaugh's careful observational work, than to Lowell's calculations.

Although the total mass of the system has been comparatively easy to determine from recent observations, the individual masses of Pluto and Charon have proven much harder to measure. The obvious approach involves the examination of the barycentric wobble of the system. This motion, however, could be expected to have an amplitude of about 0.1 arcsec, which is about an order of magnitude smaller than the orbital motion of Charon, thereby requiring even higher angular resolution observations.

In 1991 and 1992, two independent attempts were made to measure this motion, the earlier using the HST, and the latter using a groundbased telescope at a site known for its good seeing. Unfortunately, these two results, each of which has its own unique set of advantages and disadvantages, disagreed rather badly. Null et al. (1993) found the Charon–Pluto mass ratio to be 0.0837$\pm$0.0147, while Young et al. (1994) found that ratio to be 0.1566$\pm$0.0035, a difference of 4.8σ. If Pluto and Charon had equal densities, the radii derived from mutual event observations would imply a mass ratio of about 0.14 to 0.15, depending on whose radii are adopted for the calculation, thus one result favored Charon being more dense than Pluto, while the other result favored the opposite conclusion.

Because of the large discrepancy between these two measurements and the importance of having an accurate mass ratio, both teams made plans to repeat their experiments. The HST observations were repeated in 1993 (Null and Owen 1996), whereas the groundbased observations were repeated in 1995, and are currently being analyzed (Young et al. 1997). Improvements to the field distortion model used to reduce the HST data, and allowance for non-orthogonality of the rows and columns of the CCD led to a significant upward revision of the previous HST result. A solution that combined both the 1991 and 1993 data yielded a mass ratio of 0.124$\pm$0.008, though the stated uncertainty still disagrees with the original groundbased result by 3.7σ.

A further attempt to derive the mass ratio utilized center-of-light astrometry from CCD strip scans acquired to look for stellar occultation candidates. Extensive data sets acquired at Lick Observatory and Wallace Observatory in 1995 were analyzed by Foust et al. (1997), yielding 0.122±0.007 and 0.107±0.011, respectively, using the individual lightcurves measured by Buie et al. (1997) to constrain the relative contributions of each object to the total light. Less extensive data from Lick Observatory in 1993, the U.S. Naval Observatory, and the Carlsberg Automatic Meridian Circle led to a final weighted mean mass ratio of 0.117±0.006.

One other consistent, though low-precision, mass ratio determination of $0.110^{+0.063}_{-0.056}$ was found by Tholen and Buie (1997) from a series of sixty HST images acquired primarily to measure the individual rotational lightcurves of Pluto and Charon.

These mass ratio measurements are summarized in Table IV. To arrive at an adopted value, one must decide how to weight the various results. It appears doubtful that each group of authors computed their uncertainties in a consistent fashion, and in any case different techniques were used, which are subject to different sources of systematic error, so weighting by the reciprocal square of the stated uncertainty may not be appropriate. On the other hand, giving each equal weight would assign inappropriately high weight to the Tholen and Buie (1997) result, which clearly used an indirect technique. Fortunately, except for the earliest two results (whose discrepancy is partially responsible for the additional observations), the results are all reasonably consistent. For this reason, we have adopted a consensus value and uncertainty of 0.119±0.005, which spans all the recent direct measurements at the 2σ level.

TABLE IV

Summary of Mass Ratio Measurements

Dates of Observations	Charon–Pluto Mass Ratio	Reference
1991 August	0.0837±0.0147	Null et al. (1993)
1992 February–March	0.1566±0.0035	Young et al. (1994)
1992 May–1993 August	0.110±0.060	Tholen and Buie (1997)
1993 August	0.124±0.008	Null and Owen (1996)
1995 February–March	0.115[a]	Young et al. (1997)
1995 May–July	0.117±0.006	Foust et al. (1997)
Consensus value	0.119±0.005	

[a] Preliminary result.

The mean density of the Pluto–Charon system can be computed by using the total mass and the total volume occupied by the two bodies. If the mutual event radii are used to compute the volume, then it should be noted that even though the radii depend on the adopted semimajor axis for Charon's orbit, so does the mass, therefore both the mass and volume scale as the cube of the adopted semimajor axis, leaving the derived mean density unchanged.

Using the larger limb darkened radii of Young and Binzel (1994), the mean density works out to be 1.87 g cm^{-3}, while the smaller non-limb-darkened radii of Tholen and Buie (1990) or Reinsch et al. (1994) both yield a mean density of 2.03 g cm^{-3}. Using the consensus value of the mass ratio, the density of Pluto falls in the range from 1.92 to 2.06 g cm^{-3}, while the density of Charon falls in the range from 1.51 to 1.81 g cm^{-3}, based on the same three sets of radii mentioned here.

The relatively high density for Pluto indicates a composition that is not dominated by water ice, unlike many of the outer planet satellites, but rather by rock. In fact, the rock to ice ratio may be too high for an object that formed from the solar nebula at that distance from the Sun. For more details, see the chapter by McKinnon et al. The density of Triton, however, is 2.054±0.032 g cm^{-3} (Tyler et al. 1989), which is virtually identical to that of Pluto. Based on the similarity of bulk density, size, and heliocentric distance, one might expect the interior structures of Pluto and Triton to be comparable, though Triton's orbital decay heating may have produced changes not experienced by Pluto.

VII. GLOBAL SURFACE CHARACTERISTICS

The size of Pluto dictates an essentially spherical shape. The lightcurve variation must therefore be the result of surface albedo variegation, contrary to the conclusion of Hardie mentioned earlier. With one exception, all the other extraterrestrial solar system objects with brightness variations of 0.3 mag or more are comparatively small asteroids, for which nonspherical shape is the likely cause of the brightness variation with rotation. We therefore conclude that Pluto has the second most contrastive extraterrestrial surface in the solar system, exceeded only by Iapetus. The hemispherical asymmetry of Iapetus is known to coincide with the leading and trailing hemispheres of this synchronously rotating satellite of Saturn, which has led to the suggestion that infalling dark material is being preferentially swept up by the leading side of Iapetus (Cook and Franklin 1970). No such obvious mechanism exists for Pluto, however. The origin of the surface contrast on Pluto remains an open question.

The first attempt to determine the surface albedo distribution on Pluto was by Lacis and Fix (1972), who used the lightcurve inversion technique. A significantly larger data base allowed Marcialis (1983) to improve on that work, as was also the case for Buie and Tholen (1989). The first maps to benefit from mutual events observations were produced by Buie et al. (1992), followed by Reinsch et al. (1994). For considerably more detail, see the chapter by Buie et al. The first direct resolved images of Pluto were obtained with the HST by Albrecht et al. (1994), with rotationally resolved images later acquired by Stern et al. (1997). There seems to be general agreement on the existence of bright polar caps, as well as a highly variegated equatorial band.

The color of Pluto was often measured along with its brightness. Kuiper (1950) commented that Pluto's color indicated the presence of bright icy material, rather than the redder rockier material seen elsewhere in the solar system. In fact, the modern $B - V$ color index for the system is 0.84, which is significantly redder than "rocky" C-type asteroids, which tend to be neutral in color, and about as red as the least red S-type asteroids. Although no variation in the $B - V$ color index has been noted with Charon's rotation, a 0.01 mag variation was noted in the $B - V$ color for Pluto (Buie et al. 1997); variation of 0.02 and 0.03 mag was noted by Tedesco and Tholen (1980) at wavelengths of 0.70 and 0.86 μm, respectively. Confirmation of this variation was provided by Marcialis and Lebofsky (1991). The sense of the variation is such that Pluto is redder at minimum light. Grundy and Fink (1996) have also examined the variation of methane absorption strength with rotation and have proposed a three-terrain model for the surface of Pluto to explain both variations. The dark regions are proposed to be rich in organics, the brightest regions are nitrogen rich but methane poor, while the third terrain presumably contains a mixture of methane and nitrogen ices.

With the individual radii and brightnesses in hand, it is possible to compute the geometric albedos for Pluto and Charon. Of course, a single albedo value means little for Pluto, because of the large amount of albedo variation over its surface. Charon appears to be more uniform, however. Its visual geometric albedo is approximately 0.38. On average, Pluto is more reflective than Charon. To fit the mutual event data, Tholen and Buie (1990) needed to vary the blue geometric albedo of Charon-sized regions of Pluto from 0.44 to 0.61.

Pluto does vary in brightness as a function of phase angle, though that variation is rather small, due to the limited range of phase angles that an object at Pluto's distance can present. In addition, Pluto's high ecliptic latitude since discovery prevented the phase angle from getting too close to zero. The combined effects of distance and ecliptic latitude limited the observable range of phase angles to about 0.5 to 1.9 deg. Andersson and Fix (1973) were the first to attempt a determination of the phase coefficient; their result was 0.05 mag deg^{-1}. Progressively better determinations became available as more lightcurve data were amassed in the early 1980s. Marcialis (1983) found 0.031$\pm$0.006 mag deg^{-1}, Binzel and Mulholland (1984) found 0.041$\pm$0.003 mag deg^{-1}, and Tholen and Tedesco (1994) found 0.0372$\pm$0.0016 mag deg^{-1}.

Of course, all of the preceding phase coefficients refer to the combined light of the system. A determination of individual phase coefficients requires knowledge of the individual brightnesses at a variety of rotational phases and phase angles to permit those two effects to be decoupled. The first such attempt was made by Buie et al. (1997) using images from the HST; they found 0.0294$\pm$0.0011 mag deg^{-1} for Pluto and 0.0866$\pm$0.0078 mag deg^{-1} for Charon (see Fig. 4).

Pluto's current distance from the Sun implies a rather low equilibrium temperature of about 50 K. The peak of its thermal emission would be

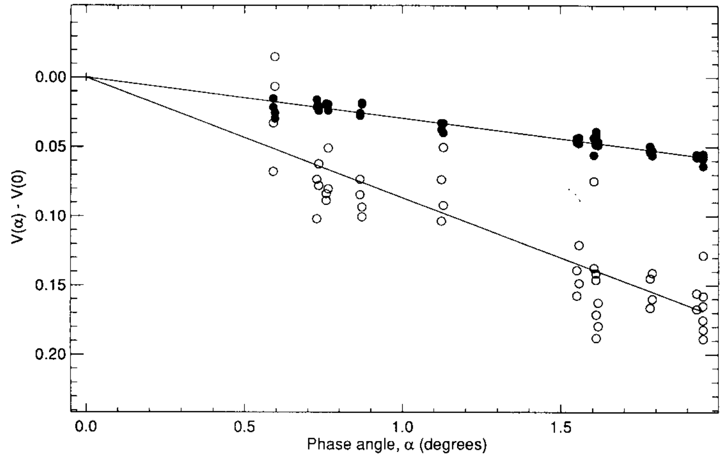

Figure 4. The phase functions of Pluto (filled circles) and Charon (open circles).

near 60 μm, which is not observable from the ground. The first temperature measurement of Pluto utilized data from the Infrared Astronomical Satellite (IRAS). The model that Sykes et al. (1987) created to explain the observations utilizes two regions, polar and equatorial, of slightly different temperature, ranging from about 52 to 59 K. Additional analyses were published by Tedesco et al. (1987) and Aumann and Walker (1987). With the advent of millimeter-wave astronomy, it became possible to detect the thermal emission from the Pluto–Charon system at these wavelengths. Altenhoff et al. (1988) made such a measurement but found a much lower temperature of 39±4 K, which has been confirmed by Stern et al. (1993) and Jewitt (1994). A rather sensitive test of temperature is provided by the shape of the nitrogen absorption band in the spectrum of Pluto. Tryka et al. (1994) used this technique to determine the temperature of the nitrogen ice on Pluto to be 40±2 K , though this result is dependent on such things as grain size (see the chapter by Spencer et al.) . This result for Pluto can be compared with Triton's, for which the same technique yielded 38±1 K. The apparent discrepancy with the IRAS temperature result can be resolved by modeling Pluto as having rather extensive polar caps of nitrogen ice and a narrow equatorial region devoid of nitrogen ice.

The surface composition of Charon was determined spectroscopically during the course of total mutual events. By subtracting the spectrum of just Pluto, obtained while Charon was completely hidden from view, from a combined spectrum of the system obtained either before or after the event, it was possible to derive a spectrum for just Charon. At wavelengths shorter than 1 μm, Charon's spectrum is essentially flat and featureless, devoid of any hint of the methane bands that are prominent in Pluto's spectrum (Fink and DiSanti 1988). Longward of 1 μm, however, are absorption features that suggest a composition of water frost (Buie et al. 1987; Marcialis et al. 1987).

Observations at wavelengths shorter than about 0.3 μm are not possible from the ground, due to absorption by terrestrial ozone. To examine this portion of the spectrum, Stern et al. (1991*a*) used the International Ultraviolet Explorer satellite to extend the spectral coverage on the Pluto–Charon system to 0.255 μm. The data revealed a rotational lightcurve that was not in phase with the one measured at longer wavelengths. The same phenomenon was not evident in a series of visible and ultraviolet images obtained with the HST (Stern et al. 1997; see also the rear cover of this book).

VIII. ATMOSPHERES

Speculation about Pluto's atmosphere began at least 46 years ago. Kuiper (1950) insisted that Pluto "must have some atmosphere," but expected most of the original atmosphere to be frozen out. He noted the absence of any excess near 0.3 μm in the spectrum of Pluto that could be caused by Rayleigh scattering and concluded that Pluto's atmospheric content is "less than 0.1 terrestrial atmospheres." Spectrophotometry by Fix et al. (1970) showed an upturn in reflectivity shortward of 0.38 μm, however, though they said nothing about a possible atmosphere being responsible for it. This upturn was not confirmed by Barker et al. (1980), who noted the difficulty of attributing any such upturn to Rayleigh scattering without knowledge of the underlying surface's albedo. More recently, Trafton and Stern (1996) used the HST to measure the ultraviolet spectrum of Pluto from 0.25 to 0.48 μm; they note the possibility of a reflectivity minimum near 0.26 μm.

Cruikshank et al. (1976) detected methane in the infrared spectrum of Pluto; Trafton (1980) used this detection and the assumption of vapor pressure equilibrium to suggest the presence of an atmosphere around Pluto, and also speculated on the presence of heavier gases as well. Fink et al. (1980) detected absorption features due to methane believed to be in the gaseous state; a one-way abundance of 27$\pm$7 m-am was inferred. Additional rotationally resolved observations of Pluto's spectrum revealed variation in the methane band strength, indicating that a portion of the absorption must be due to methane frost on the surface, thereby reducing the amount of gas necessary to reproduce the spectrum to about 5.5 m-am (Buie and Fink 1987).

The spectral evidence is somewhat circumstantial, due to the difficulty in distinguishing between gaseous and solid methane absorptions. Stellar occultations provide a more direct method for detecting atmospheres of planets. Unfortunately, stellar occultations involving Pluto are fairly rare, as noted in Sec. V. The first stellar occultation by Pluto to be observed was in 1985 (Brosch 1995). The conditions were far from ideal, unfortunately, with both clouds and flares from nearby military forces showing up in the data, making interpretation difficult. The event was of relatively short duration, indicating only grazing geometry, but the decline and recovery of the stellar signal was far too gradual to be due to a stellar disk disappearing and reappearing from behind the solid surface of the occulting body. The presence of an atmosphere was inferred, though sufficient uncertainty remained, due to the adverse conditions (see the chapter by Binzel and Hubbard for more detail).

Conclusive evidence for an atmosphere around Pluto came in 1988 when, for the first time, multiple sites observed an occultation by Pluto (Millis et al. 1993). The highest quality data set was obtained from the Kuiper Airborne Observatory and was initially analyzed by Elliot et al. (1989). They determined the ratio of the atmospheric temperature to mean molecular weight to be 4.2±0.4 K amu^{-1}. Because methane had been detected spectroscopically, and the molecular weight of methane is 16 amu, an atmospheric temperature of about 67±6 K could be deduced, which is not too much greater than the temperature of 53 to 59 K deduced by Sykes et al. (1987) from radiometric observations obtained by the IRAS. Elliot et al. also considered the possibility of a nitrogen atmosphere, which would have required a temperature of 117±11 K.

Yelle and Lunine (1989) noted that methane would absorb solar infrared radiation, thereby raising the temperature of a methane atmosphere to as high as 106 K near the 1 μbar pressure level, and used that information to deduce a mean molecular weight of 25±3 amu for Pluto's atmosphere, which implies the presence of a heavier gas. Spectroscopic evidence for the presence of a heavier gas was provided by Owen et al. (1993), who used new infrared detector technology to discover the signatures of molecular nitrogen and carbon monoxide in Pluto's spectrum. Models of that spectrum yielded estimates that nitrogen is about 50 times more abundant than either of the other two ices. In addition, because the vapor pressure of nitrogen is so much higher than for either carbon monoxide or methane, nitrogen is presumed to be the primary atmospheric constituent. They also note, however, that the cosmic abundance of neon is comparable to that of nitrogen and speculate that if present, neon could dominate the atmosphere.

Another unique characteristic of Pluto's atmosphere is that it is hydrodynamically escaping. For more details, see the chapter by Trafton et al.

The surface pressure of Pluto's atmosphere is not well determined, due to the uncertainty regarding the depth to which the occultation measurements probed. Tryka et al. (1994) note that at the temperature they found for the nitrogen ice from the spectral band shape, vapor pressure equilibrium would imply a surface pressure of approximately 60 μbar, which is significantly higher than the 3 to 10 μbar pressures deduced by Yelle and Lunine (1989) and Hubbard et al. (1990). A possible explanation is provided by the troposphere model of Stansberry et al. (1994).

Given that Pluto has such a thin atmosphere and that Charon's gravity is even weaker than Pluto's, one might not expect Charon to have an atmosphere of its own. Nevertheless, Elliot and Young (1991) can find no other likely explanation for the occultation lightcurve observed by Walker (1980). If the satellite were truly atmosphereless, then the star should have disappeared quite abruptly, yet one sample point preceding the event and one point following show statistically significant departure from the unocculted brightness level. The authors speculate on the possibility that these features were caused by an atmosphere, though little can be done with the data, other than to place upper limits on the amounts of various candidate gases.

IX. CONCLUSIONS

Our knowledge of the Pluto–Charon system has grown tremendously during the past two decades, yet several questions remain. Although the orbital semimajor axis for Charon, which is needed to scale the mutual event radius models, is no longer a significant source of error in those determinations, there are still some uncomfortably large differences in the orbital inclination measurements, which affect the accuracy of the obliquity determination, and in turn the average insolation for a given point on Pluto's surface. Of perhaps more immediate interest is the surprising eccentricity signature in the HST data. How much can be attributed to surface albedo effects? If a significant nonzero amount remains, what either caused it or sustains it? Might the spin axis of Pluto be slightly nonparallel to Charon's orbital angular momentum vector as well?

How much is the rotational period determination for Pluto affected by surface albedo features? What is the rotational period of Charon? Is it synchronous as expected? We have gone from only speculating about the size of Pluto to measurements that involved debates at the 1000 km level, to debates now at the 10 km level. A determination of the amount of limb darkening appears necessary to resolve the current discrepancy between mutual event and stellar occultation measurements.

Early in the preparation of this chapter, there was still an outstanding question about the Charon–Pluto mass ratio, but there are now indications of this problem having been solved. What is the origin of the extreme surface contrast on Pluto? Is the albedo pattern static, or dynamic in response to volatile transport?

The true atmospheric structure is still unknown. Is the atmosphere clear, or is a haze layer present? Does Pluto have a troposphere? Better radius determinations from the mutual events may help favor one of these models. In what proportions do nitrogen, carbon monoxide, and methane appear? Does Charon have a detectable atmosphere? With Pluto's galactic latitude currently decreasing, we can anticipate a higher probability of suitable stellar occultation candidates being found that can allow these questions to be answered, and to look also for the expected temporal variability in atmospheric bulk. Obviously, much more work can be done, and we can look forward to another couple of decades of exciting discoveries about this intriguing system.

Acknowledgments. This chapter would not have been possible without the able assistance of M. S. Matthews and A. Schumann-Ruskin. The scientific content benefitted from reviews by R. Binzel, W. Hubbard, and especially

J. Elliot. A portion of the work presented here was supported by a grant from NASA.

REFERENCES

Albrecht, R., Barbieri, C., Adorf, H.-M., Corrain, G., Gemmo, A., Greenfield, P., Hainaut, O., Hook, N., Tholen, D. J., Blades, J. C., and Sparks, W. B. 1994. High-resolution imaging of the Pluto–Charon system with the Faint Object Camera of the Hubble Space Telescope. *Astrophys. J. Lett.* 435:75–78.

Altenhoff, W. J., Chini, R., Hein, H., Kreysa, E., Mezger, P. G., Salter, C., and Schraml, J. B. 1988. First radio astronomical estimate of the temperature of Pluto. *Astron. Astrophys.* 190:L15–L17.

Andersson, L. E. 1978. Eclipse phenomena of Pluto and its satellite. *Bull. Amer. Astron. Soc.* 10:586 (abstract).

Andersson, L. E., and Fix, J. D. 1973. Pluto: New photometry and a determination of the axis of rotation. *Icarus* 20:279–283.

Anonymous. 1965. American astronomers report. *Sky & Tel.* 29:141.

Anonymous. 1992. Reference. In *Explanatory Supplement to the Astronomical Almanac*, ed. P. K. Seidelmann (Mill Valley, Calif.: University Science Books), pp. 693–719.

Applegate, J. H., Douglas, M. R., Gürsell, Y., Sussman, G. J., and Wisdom, J. 1986. The outer solar system for 200 million years. *Astron. J.* 92:176–194.

Arnold, S. J., Boksenberg, A., and Sargent, W. L. W. 1979. Measurement of the diameter of Pluto by speckle interferometry. *Astrophys. J. Lett.* 234:159–163.

Aumann, H. H., and Walker, R. G. 1987. IRAS observations of the Pluto–Charon system. *Astron. J.* 94:1088–1091.

Baade, W. 1934. The photographic magnitude and color index of Pluto. *Publ. Astron. Soc. Pacific* 46:218–221.

Baier, G., and Weigelt, G. 1987. Speckle interferometric observations of Pluto and its moon Charon on seven different nights. *Astron. Astrophys.* 174:295–298.

Barker, E. S., Cochran, W. D., and Cochran, A. L. 1980. Spectrophotometry of Pluto from 3500 to 7350 Å. *Icarus* 44:43–52.

Beletic, J. W., Goody, R. M., and Tholen, D. J. 1989. Orbital elements of Charon from speckle interferometry. *Icarus* 79:38–46.

Binzel, R. P., and Mulholland, J. D. 1983. Photometry of Pluto during the 1982 opposition. *Astron. J.* 88:222–225.

Binzel, R. P., and Mulholland, J. D. 1984. Photometry of Pluto during the 1983 opposition: A new determination of the phase coefficient. *Astron. J.* 89:1759–1761.

Bonneau, D., and Foy, R. 1980. Speckle interferometry with the CFHT 3.60 m. I. Resolution of the system Pluto–Charon. *Astron. Astrophys.* 92:L1–L4.

Bosh, A. S., Young, L. A., Elliot, J. L., Hammel, H. B., and Baron, R. L. 1992. Photometric variability of Charon at 2.2 μm. *Icarus* 95:319–324.

Brosch, N. 1995. The 1985 stellar occultation by Pluto. *Mon. Not. Roy. Astron. Soc.* 276:571–578.

Buie, M. W., and Fink, U. 1987. Methane absorption variations in the spectrum of Pluto. *Icarus* 70:483–498.

Buie, M. W., and Shriver, S. K. 1994. The distribution of water frost on Charon. *Icarus* 108:225–233.

Buie, M. W., and Tholen, D. J. 1989. The surface albedo distribution of Pluto. *Icarus* 79:23–37.

Buie, M. W., Cruikshank, D. P., Lebofsky, L. A., and Tedesco, E. F. 1987. Water frost on Charon. *Nature* 329:522–523.

Buie, M. W., Tholen, D. J., and Horne, L. 1992. Albedo maps of Pluto and Charon: Initial mutual event results. *Icarus* 97:211–227.

Buie, M. W., Tholen, D. J., and Wasserman, L. H. 1997. Separate lightcurves of Pluto and Charon. *Icarus* 125:233–244.

Buratti, B. J., Dunbar, R. S., Tedesco, E. F., Gibson, J., Marcialis, R. L., Wong, F., and Bennett, S. 1995. Modeling Pluto–Charon mutual events. II. CCD observations with the 60 in. telescope at Palomar Mountain. *Astron. J.* 110:1405–1419.

Christy, J. W., and Harrington, R. S. 1978. The satellite of Pluto. *Astron. J.* 83:1005–1008.

Cohen, C. J., and Hubbard, E. C. 1965. Libration of the close approaches of Pluto to Neptune. *Astron. J.* 70:10–13.

Cook, A. F., and Franklin, F. A. 1970. An explanation of the light curve of Iapetus. *Icarus* 13:282–291.

Cruikshank, D. P., Pilcher, C. B., and Morrison, D. 1976. Pluto: Evidence for methane frost. *Science* 194:835–837.

Dessler, A. J., and Russell, C. T. 1980. From the ridiculous to the sublime: The pending disappearance of Pluto. *Eos: Trans. AGU* 61:691.

Dunbar, R. S., and Tedesco, E. F. 1986. Modeling Pluto-Charon mutual eclipse events. I. First-order models. *Astron. J.* 92:1201–1209.

Duncombe, R. L., and Seidelmann, P. K. 1980. A history of the determination of Pluto's mass. *Icarus* 44:12–18.

Elliot, J. L., and Young, L. A. 1991. Limits on the radius and a possible atmosphere of Charon from its 1980 stellar occultation. *Icarus* 89:244–254.

Elliot, J. L., and Young, L. A. 1992. Analysis of stellar occultation data for planetary atmospheres. I. Model fitting, with application to Pluto. *Astron. J.* 103:991–1015.

Elliot, J. L., Dunham, E. W., Bosh, A. S., Slivan, S. M., Young, L. A., Wasserman, L. H., and Millis, R. L. 1989. Pluto's atmosphere. *Icarus* 77:148–170.

Farinella, P., Milani, A., Nobili, A. M., and Valsecchi, G. B. 1979. Tidal evolution and the Pluto–Charon system. *Moon and Planets* 20:415–421.

Fink, U., and DiSanti, M. A. 1988. The separate spectra of Pluto and its satellite Charon. *Astron. J.* 95:229–236.

Fink, U., Smith, B. A., Benner, D. C., Johnson, J. R., Reitsema, H. J., and Westphal, J. A. 1980. Detection of a CH_4 atmosphere on Pluto. *Icarus* 44:62–71.

Fix, J. D., Neff, J. S., and Kelsey, L. A. 1970. Spectrophotometry of Pluto. *Astron. J.* 75:895–896.

Foust, J. A., Elliot, J. L., Olkin, C. B., McDonald, S. W., Dunham, E. W., Stone, R. P. S., McDonald, J. S., and Stone, R. C. 1997. Determination of the Charon-Pluto mass ratio from center-of-light astrometry. *Icarus*, in press.

Grundy W. M., and Fink, U. 1996. Synoptic CCD spectrophotometry of Pluto over the past 15 years. *Icarus* 124:329–343.

Halliday, I., Hardie, R. H., Franz, O. G., and Priser, J. B. 1966. An upper limit for the diameter of Pluto. *Publ. Astron. Soc. Pacific* 78:113–124.

Hardie, R. 1965. A re-examination of the light variation of Pluto. *Astron. J.* 70:140.

Harrington, R. S., and Christy, J. W. 1980. The satellite of Pluto. II. *Astron. J.* 85:168–170.

Harrington, R. S., and Christy, J. W. 1981. The satellite of Pluto. III. *Astron. J.* 86:442–443.

Hubbard, W. B., Yelle, R. V., and Lunine, J. I. 1990. Nonisothermal Pluto atmosphere models. *Icarus* 84:1–11.

Jewitt, D. C. 1994. Heat from Pluto. *Astron. J.* 107:372–378.

Kiladze, R. I. 1966. On the rotation period of Pluto. *Byull. Abastuman. Astrofiz. Obs.* 34:131–133.

Kuiper, G. P. 1950. The diameter of Pluto. *Publ. Astron. Soc. Pacific* 62:133–137.

Lacis, A. A., and Fix, J. D. 1972. An analysis of the light curve of Pluto. *Astrophys. J.* 174:449–453.

Lyutyi, V. M., and Tarashchuk, V. P. 1982. A photometric study of Pluto near perihelion. I. U,B,V photometry. *Soviet Astron. Lett.* 8:56–59.

Lyutyi, V. M., and Tarashchuk, V. P. 1984. A photometric study of Pluto near perihelion. II. Rotation period and color indices. *Soviet Astron. Lett.* 10:226–229.

Malhotra, R. 1995. The origin of Pluto's orbit: Implications for the solar system beyond Neptune. *Astron. J.* 110:420–429.

Marcialis, R. L. 1983. A Two-Spot Model for the Surface of Pluto. Master's Thesis, Vanderbilt University.

Marcialis, R. L. 1985. Topographic relaxation on ice covered worlds: Application to Pluto. *Bull. Amer. Astron. Soc.* 17:715 (abstract).

Marcialis, R. L., and Lebofsky, L. A. 1991. CVF spectrophotometry of Pluto: Correlation of composition with albedo. *Icarus* 89:255–263.

Marcialis, R. L., Rieke, G. H., and Lebofsky, L. A. 1987. The surface composition of Charon: Tentative identification of water ice. *Science* 237:1349–1351.

Millis, R. L., Wasserman, L. H., Franz, O. G., Nye, R. A., Elliot, J. L., Dunham, E. W., Bosh, A. S., Young, L. A., Slivan, S. M., Gilmore, A. C., Kilmartin, P. M., Allen, W. H., Watson, R. D., Dieters, S. W., Hill, K. M., Giles, A. B., Blow, G., Priestley, J., Kissling, W. M., Walker, W. S. G., Marino, B. G., Dix, D. G., Page, A. A., Ross, J. E., Avey, H. P., Hickey, D., Kennedy, H. D., Mottram, K. A., Moyland, G., Murphy, T., Dahn, C. C., and Klemola, A. R. 1993. Pluto's radius and atmosphere: Results from the entire 9 June 1988 occultation data set. *Icarus* 105:282–297.

Neff, J. S., Lane, W. A., and Fix, J. D. 1974. An investigation of the rotational period of the planet Pluto. *Publ. Astron. Soc. Pacific* 86:225–230.

Null, G. W., and Owen, W. M. Jr. 1996. Charon/Pluto mass ratio obtained with HST CCD observations in 1991 and 1993. *Astron. J.* 111:1368–1381.

Null, G. W., Owen, W. M., Jr., and Synnott, S. P. 1993. Masses and densities of Pluto and Charon. *Astron. J.* 105:2319–2335.

Owen, T. C., Roush, T. L., Cruikshank, D. P., Elliot, J. L., Young, L. A., de Bergh, C., Schmitt, B., Geballe, T. R., Brown, R. H., and Bartholomew, M. J. 1993. Surface ices and the atmospheric composition of Pluto. *Science* 261:745–748.

Owen, T. C., Cruikshank, D. P., Roush, T., Geballe, T. R., and de Bergh, C. 1997. Water ice on Pluto. In preparation.

Reinsch, K., Burwitz, V., and Festou, M. C. 1994. Albedo maps of Pluto and improved physical parameters of the Pluto–Charon system. *Icarus* 108:209–218.

Reitsema, H. J., Vilas, F., and Smith, B. A. 1983. A charge-coupled device observation of Charon. *Icarus* 56:75–79.

Standish, E. M., Jr. 1993. Planet X: No dynamical evidence in the optical observations. *Astron. J.* 105:2000–2006.

Stansberry, J. A., Lunine, J. I., Hubbard, W. B., Yelle, R. V., and Hunten, D. M. 1994. Mirages and the nature of Pluto's atmosphere. *Icarus* 111:503–513.

Stern, S. A., Brosch, N., Barker, E. S., and Gladstone, G. R. 1991*a*. Rotationally resolved midultraviolet studies of Triton and the Pluto/Charon system. I. IUE results. *Icarus* 92:332–341.

Stern, S. A., Fesen, R. A., Barker, E. S., Parker, J. W., and Trafton, L. M. 1991*b*. A search for distant satellites of Pluto. *Icarus* 94:246–249.

Stern, S. A., Weintraub, D. A., and Festou, M. C. 1993. Evidence for a low surface temperature on Pluto from millimeter-wave thermal emission measurements. *Science* 261:1713–1716.

Stern, S. A., Parker, J. W., Duncan, M. J., Snowdall, Jr., J. C., and Levison, H. F. 1994. Dynamical and observational constraints on satellites in the inner Pluto–Charon system. *Icarus* 108:234–242.

Stern, S. A., Buie, M. W., and Trafton, L. M. 1997. HST high-resolution images and maps of Pluto. *Astron. J.* 113:827–843.

Sussman, G. J., and Wisdom, J. 1988. Numerical evidence that the motion of Pluto is chaotic. *Science* 241:433–437.

Sykes, M. V., Cutri, R. M., Lebofsky, L. A., and Binzel, R. P. 1987. IRAS serendipitous survey observations of Pluto and Charon. *Science* 237:1336–1340.

Tedesco, E. F., and Tholen, D. J. 1980. Photometric observations of Pluto in 1980. *Bull. Amer. Astron. Soc.* 12:729 (abstract).

Tedesco, E. F., Veeder, G. J., Jr., Dunbar, R. S., and Lebofsky, L. A. 1987. IRAS constraints on the sizes of Pluto and Charon. *Nature* 327:127–129.

Tholen, D. J. 1985. The orbit of Pluto's satellite. *Astron. J.* 90:2353–2359.

Tholen, D. J., and Buie, M. W. 1989. Further analysis of Pluto-Charon mutual event observations—1989. *Bull. Amer. Astron. Soc.* 21:981–982 (abstract).

Tholen, D. J., and Buie, M. W. 1990. Further analysis of Pluto–Charon mutual event observations—1990. *Bull. Amer. Astron. Soc.* 22:1129 (abstract).

Tholen, D. J., and Buie, M. W. 1997. The orbit of Charon. I. New Hubble Space Telescope observations. *Icarus* 125:245–260.

Tholen, D. J., and Tedesco, E. F. 1994. Pluto's lightcurve: Results from four oppositions. *Icarus* 108:200–208.

Trafton, L. 1980. Does Pluto have a substantial atmosphere? *Icarus* 44:53–61.

Trafton, L. M., and Stern, S. A. 1996. Rotationally resolved spectral studies of Pluto from 2500 to 4800 Åobtained with HST. *Astron. J.* 112:1212–1224.

Tryka, K. A., Brown, R. H., Cruikshank, D. P., Owen, T. C., Geballe, T. R., and de Bergh, C. 1994. Temperature of nitrogen ice on Pluto and its implications for flux measurements. *Icarus* 112:513–527.

Tyler, G. L., Sweetnam, D. N., Anderson, J. D., Borutzki, S. E., Campbell, J. K., Eshleman, V. R., Gresh, D. L., Gurrola, E. M., Hinson, D. P., Kawashima, N., Kursinski, E. R., Levy, G. S., Lindal, G. F., Lyons, J. R., Marouf, E. A., Rosen, P. A., Simpson, R. A., and Wood, G. E. 1989. Voyager radio science observations of Neptune and Triton. *Science* 246:1466–1473.

Walker, A. R. 1980. An occultation by Charon. *Mon. Not. Roy. Astron. Soc.* 192:47P–50P.

Walker, M. F., and Hardie, R. 1955. A photometric determination of the rotational period of Pluto. *Publ. Astron. Soc. Pacific* 67:224–231.

Yelle, R. V., and Lunine, J. I. 1989. Evidence for a molecule heavier than methane in the atmosphere of Pluto. *Nature* 339:288–290.

Young, E. F., and Binzel, R. P. 1994. A new determination of radii and limb parameters for Pluto and Charon from mutual event lightcurves. *Icarus* 108:219–224.

Young, L. A., Olkin, C. B., Elliot, J. L., Tholen, D. J., and Buie, M. W. 1994. The Charon–Pluto mass ratio from MKO astrometry. *Icarus* 108:186–199.

Young, L. A., Tholen, D. J., Buie, M. W., and Olkin, C. B. 1997. The Charon/Pluto mass ratio from 1995 MKO observations. *Icarus*, in preparation.

PLUTO
AND
CHARON

S. Alan Stern
David J. Tholen

Editors

With the editorial assistance of
A. S. Ruskin, M. L. Guerrieri and M. S. Matthews

With 50 collaborating authors

THE UNIVERSITY OF ARIZONA PRESS
Tucson